

NMR spectroscopy study of local correlations in water

Francesco Mallamace,^{1,2,3,a)} Carmelo Corsaro,² Domenico Mallamace,⁴ Sebastiano Vasi,¹ and H. Eugene Stanley³

¹*Dipartimento MIFT, Sezione di Fisica, Università di Messina, I-98166 Messina, Italy*

²*Consiglio Nazionale delle Ricerche-IPCF Messina, I-98158 Messina, Italy*

³*Center for Polymer Studies and Department of Physics, Boston University, Boston, Massachusetts 02215, USA*

⁴*Consorzio Interuniversitario per lo Sviluppo dei Sistemi a Grande Interfase - CSGI, Sesto Fiorentino, Firenze 50019, Italy*

(Received 22 September 2016; accepted 11 November 2016; published online 5 December 2016)

Using nuclear magnetic resonance we study the dynamics of the hydrogen bond (HB) sub-domains in bulk and emulsified water across a wide temperature range that includes the supercooled regime. We measure the proton spin-lattice T_1 and spin-spin T_2 relaxation times to understand the hydrophilic interactions that determine the properties of water. We use (i) the Bloembergen, Purcell, and Pound approach that focuses on a single characteristic correlation time τ_c , and (ii) the Powles and Hubbard approach that measures the proton rotational time τ_θ . We find that when the temperature is low both relaxation times are strongly correlated when the HB lifetime is long, and that when the temperature is high a decrease in the HB lifetime destroys the water clusters and decouples the dynamic modes of the system. *Published by AIP Publishing.* [<http://dx.doi.org/10.1063/1.4968589>]

I. INTRODUCTION

Water is an interesting and intriguing research subject that is essential to life and human activity but we still do not completely understand its behavior.^{1,2} This apparently simple molecule of two atoms of hydrogen and one of oxygen has many anomalous thermodynamical properties, e.g., the density maximum at 4 °C. The most puzzling of these anomalies are the significant increases in volume, entropy fluctuations, and cross-fluctuations when the temperature is decreased down to the supercooled state—a moderate pressure allows supercooling down to approximately 180 K.^{3,4} (In normal liquids, fluctuations decrease when T is decreased.) In addition, such transport quantities as thermal conductivity, viscosity, self-diffusion, and relaxation times all display anomalies.^{5–10} There are thus many open questions regarding the chemical-physical properties of water, both dynamic and structural.

Although these anomalies are found in the low T region of the water phase diagram, the high T regime of the stable liquid is also of interest, in particular in water solutions and in water in biological systems. Hydrogen bond (HB) interactions determine the properties of water in both bulk and solution configurations. Each water molecule has two positively charged lobes containing the protons and two lone pairs of electrons. The HB is a non-covalent interaction between an electropositive hydrogen atom on one molecule and an electronegative oxygen atom on a second molecule.

The tetrahedral symmetry of the local order around each water molecule generates anticorrelations in the supercooled state.² As water is cooled, the HB interaction orders the nearest neighbor molecules that gradually assume the four-coordinated geometry characteristic of the local structure of water. In ordinary ice, each water molecule has four nearest

neighbors, a hydrogen donor to two of them and a hydrogen receptor from the other two. Also in the liquid phase water is governed by tetrahedrality, but in contrast to the solid crystalline phase with a permanent network held together by HB, it is local and transient. Regions of local tetrahedral order can possess a larger specific volume than the overall average. The entropy, on the other hand, always decreases upon cooling because the specific heat is, of necessity, positive. As T decreases, the local specific volume increases due to the progressive increase in the tetrahedral order. Thus the entropy and volume can become anticorrelated, and the thermal expansion coefficient $\alpha_P = -(\partial \ln \rho / \partial T)_P$ can become negative. Water studies of the thermodynamical response functions suggest that when the temperature is decreased the onset of the tetrahedral water patches occurs at $T^* \approx 320$ K. At higher temperatures, the behavior of water is the same as in simple liquids.¹¹

When water is in a solution, the solute chemical moieties change the HB ordering process, e.g., the ion charge in salt solutions and the hydrophobic heads in simple alcohols and polymer systems. The functions of biosystems, e.g., peptides, proteins, or DNA, are affected by their interaction with water and in particular by the contrast between hydrophilic and hydrophobic metabolites. Thus water is not simply a solvent but is also an integral and active component, i.e., it is itself an important “biomolecule” that plays both a dynamic and structural role.¹²

Water interactions—both hydrophilic (HBs) and hydrophobic—are thus key in understanding the properties of water and how water functions in biological environments.¹³ Using nuclear magnetic resonance (NMR) experiments it was recently found that, in the thermal denaturation of hydrated lysozyme, the hydrophilic (the amide NH) and hydrophobic (methyl CH₃ and methine CH) peptide groups evolve and exhibit different temperature behaviors, thus clarifying the role

^{a)}Electronic mail: francesco.mallamace@unime.it

of water and hydrogen bonding in the stabilization of protein configurations.¹⁴

Although HB interactions have been well described both experimentally and theoretically, hydrophobicity remains an open question, e.g., we do not know the potential form of the mean hydrophobic force. We also do not know the conformation of the water molecules in the hydration shells around a hydrophobic solute or what contributes to its entropy and to the energy of the change in the structure of the solute itself. We only know the solute effect of neighboring water on the structure.

Here we use the measured relaxation time as a function of temperature to examine the HB properties of bulk water. Using a ¹H NMR experiment we measure both the proton spin-lattice relaxation time (T_1) and the proton spin-spin relaxation time (T_2) to quantify water properties across temperatures that range from the stable liquid phase to the supercooled phase, and hence the time required for a molecule to interact. Originally T_1 was defined as the time required after a constant field H_0 is applied for thermal equilibrium to be established. Although T_1 is the time required for energy to be transferred by a molecule to its environment at a resonance frequency (the shorter the time, the stronger the interaction),^{15,16} T_2 is the time required for the transverse component of the magnetization to disappear due to dephasing mechanisms provoked by the interaction between spins of the same species (as in T_1 , the shorter the T_2 , the stronger the interaction).

An important property of solid water is polymorphism.^{17,18} Subject to both T and P , water has two amorphous (glassy) phases with differing structures, low density amorphous (LDA) and high density amorphous (HDA) ice. LDA can be formed from HDA and vice versa.^{19–21} Current models explaining the behavior of liquid bulk water, e.g., the relationship between supercooled and glassy water and the nature of the transition between the two glassy phases LDA and HDA, are based on polymorphism. Three hypotheses are of interest: (i) the stability limit conjecture, (ii) the singularity-free scenario (SF), and (iii) the liquid-liquid phase transition (LLPT) hypothesis. The latter two assume that water properties are the result of intermolecular HBs forming a locally structured transient gel comprised of many molecules that increase in number as the temperature decreases.^{22,23} These local “patches” or HB sub-domains^{24,25} enhance the fluctuations in specific volume and entropy and their negative cross correlations with anomalies that closely resemble those observed experimentally. In addition, the two amorphous states are the corresponding vitreous forms of low-density liquid (LDL) and high-density liquid (HDL). Upon supercooling, the response functions increase sharply but remain finite in the SF case. In the LLPT, there is a transition with critical fluctuations. Here we will use the NMR spectroscopy technique to study the thermal evolution of the dynamics of these local HB “patches” in order to better understand the properties of the hydrophilic interaction.

II. MATERIALS AND EXPERIMENTAL METHODS

A. Samples

We study bulk and emulsified water at a pressure of 1 bar. We studied bulk water in the 373–263 K temperature range,

and emulsified water in the $310 > T > 238$ K range for both T_1 and T_2 . For T_1 we also studied a larger temperature interval by heating the samples to 332 K. The accuracy throughout the experiments was ± 0.02 K. We constructed the water emulsion with water droplets of a size range 1–10 μm by using a homogenizer to stir 4000 mg of de-ionized water (H_2O) in a matrix of 2000 mg methylcyclohexane, 2000 mg methylcyclopentane, and 200 mg sorbitan tristearate. We used the same emulsion employed for a water density study in the deep supercooled regime²⁶ and for an NMR experiment about T_1 as a function of pressure.²⁷

For the NMR experiments, we used a Bruker Avance spectrometer operating at 700 MHz. The pulse sequence used to measure T_1 was the inversion recovery by varying the interpulse delay from microseconds to several seconds. For the spin-spin relaxation, we used the Carr-Purcell-Meiboom-Gill procedure.²⁸

B. Results and data analysis

The pioneering work of Bloch, Purcell and their collaborators^{15,29} describes the broadening of the spectral lines and the relaxation effects of condensed phases in NMR absorption. A complete theoretical treatment, relatively simple when the fields on each of the magnetic moments are independent, becomes complicated when these moments are directly or indirectly coupled and their fields correlated (e.g., as in dipolar and exchange interactions).

One of the first attempts to explore experimental NMR data was proposed by Bloembergen, Purcell, and Pound (BPP). They consider how energy is transferred from a radiofrequency circuit to a system of nuclear spins immersed in a magnetic field H_0 by transitions among the energy levels of the spin system when the spins are non-interacting.¹⁵ System exposure to the perturbing radiation, with consequent energy exchanges, upsets the original equilibrium state by equalizing the populations of the various levels. The new equilibrium state is due to the effects of the radiofrequency field and is a balance between the absorption of energy by the spins from the radiation field and the transfer of energy to the heat reservoir supplied by all other internal degrees of freedom in the substance containing the nuclei.

This process is the so-called spin-lattice interaction described by a characteristic spin-lattice relaxation time T_1 . This relaxation time also measures how long one must wait after the application of the constant field H_0 for the establishment of thermal equilibrium. The competition between resonance absorption and spin-lattice interaction mentioned above also provides a way of measuring T_1 .

The BPP approach thus proposes that the effect of the nuclear motion on the dipolar broadening can be treated as a random modulation of the dipolar field caused by the Brownian motion of the atomic nuclei. Under these conditions, by assuming that the intermolecular effects are negligible (or absent as in an ideal fluid) and the system is dominated by the dipole-dipole interaction, it follows that¹⁵

$$\frac{1}{T_1} = \frac{3}{2} \gamma^4 \hbar^2 I(I+1) \left[J_1(\nu_0) + \frac{1}{2} J_2(2\nu_0) \right], \quad (1)$$

where γ is the gyromagnetic ratio of proton, $2\pi\hbar$ is the Planck constant, I are the spin energy levels, $\omega_0/2\pi = \nu_0$ is the Larmor frequency, and J_i indicates the spectral components (Lorentzians). Here $1/T_1$ can be divided into two parts ($1/T_1 = (1/T_1)_{\nu_0} + (1/T_1)_{2\nu_0}$) corresponding to the single-spin and double-spin inversion processes, and each part is expressed by the corresponding J_N .

This result was applied to water by focusing on how a given proton is affected by its nearest neighbor (the other proton in the H_2O molecule), by assuming that the molecule is rigid, and by assuming that the orientation and direction of the vector connecting the two protons varies randomly. Here the ^1H T_1 measured in water is determined by the interaction fluctuations induced by molecular motions that are characterized by a correlation time τ_c and that are the result of the thermal motion of the magnetic nuclei affecting the spin-spin interaction. This is associated with the local Brownian motion and is closely related to the characteristic time that occurs in the Debye theory of polar liquids as

$$\frac{1}{T_1} = \frac{3}{10} \frac{\gamma^4 \hbar^2}{r^6} \left[\frac{\tau_c}{1 + \omega_0^2 \tau_c^2} + \frac{4\tau_c}{1 + 4\omega_0^2 \tau_c^2} \right], \quad (2)$$

where r is the interproton distance. There is also a relation between τ_c and the nuclear Larmor frequency when this latter quantity is much less than $1/T_1$, averaging out the perturbations caused by the local field. In this case, the width of the frequency resonance line is $\sim \tau_c$.

The problem of magnetic resonance absorption was recently reconsidered and a general expression for the frequency-dependent susceptibility of a magnetic system obtained using a quantum-statistical method based on the linear theory of irreversible process that uses projection operators.¹⁶ Here the relaxation or the self-correlation function of the magnetic moment (i.e., the Fourier transform of the absorption intensity distribution) is expanded by assuming that the perturbation energy changes the distribution of the resonance spectrum. We consider the system Hamiltonian to be the sum of a “secular” term that commutes with the unperturbed terms and a “non-secular” portion of the perturbation. Secular and non-secular contributions lead to different relaxation functions with different relaxation times. Thus the different J_N spectral functions are characterized by different τ_i . Only when the relaxation function is assumed to be a single exponential, the system can be described by a single relaxation time (τ_c). In the ideal case of isotropic nuclear arrangements, the two kinds of spin inversion processes have different weights for the spin-lattice relaxation (that in this latter model is $1/T_1 = 3/2\gamma^4\hbar^2 I(I+1) [J_1(\nu_0) + J_2(2\nu_0)]$) and the non-secular broadening effect ($1/T_1' = \gamma^4\hbar^2 I(I+1) [15/4J_1(\nu_0) + 3/8J_2(2\nu_0)]$), so that they are generally not identical. The model also produces a different relation for the spin-spin relaxation time T_2 ($1/T_2 = \gamma^4\hbar^2 I(I+1)\tau_0 + 1/T_1'$), which in the ideal case in which all the relaxation times corresponding to the different spectral functions are identical to τ_c , which is given by

$$\frac{1}{T_2} = \frac{3\gamma^4\hbar^2}{20r^6} \left[3\tau_c + \frac{5\tau_c}{1 + \omega_0^2\tau_c^2} + \frac{2\tau_c}{1 + 4\omega_0^2\tau_c^2} \right]. \quad (3)$$

Finally, in the limit of the rapid decrease of the correlations where the secular width is strongly narrowed and the non-secular broadening slight, $1/\omega_0 \gg \tau_c$. When the nuclear arrangement is isotropic it is $T_2\tau_c \sim \text{const.}$ and $T_2 \approx T_1$.

It is thus clear that in a real system in which the spin interactions and correlations at molecular level are effective, the experimental behavior will vary in a way not fully accounted for in these models. It is also possible that the spin magnetization when the liquid returns to equilibrium will not be exponential. Examples include water with its complex thermodynamics and systems characterized by strong correlations or clustering processes, e.g., many of those that are supercooled. Here T_1 must reflect the significant fluctuating interactions between the spin and the rest of the material of which the nucleus is a part.

We thus use the BPP approach on bulk and emulsified water and the measured T_1 and T_2 to obtain the correlation time τ_c and to study their evolutions as a function of τ_c inside the stable liquid and the supercooled metastable liquid. Figure 1 shows the behaviors of the spin-lattice T_1 and spin-spin T_2 in an Arrhenius plot (i.e., the log of T_1 and T_2 (s) vs $1000/T$ (K^{-1})), measured in the experiment (open symbols) and the literature data.^{30,31} Note that the temperature behaviors of these two relaxation times of bulk and emulsified water show, within the experimental error, that water inside micrometer droplets behaves like bulk water. Although in the stable phase these nuclear absorption times have a different temperature dependence immediately below the melting temperature ($T_M = 273.16$ K), inside the supercooled phase their behaviors are approximately the same. Figure 2 shows another Arrhenius plot of the correlation time τ_c calculated from the experimental values of T_1 and T_2 according to the BPP model and by considering the quantity T_1/T_2 . Note that this correlation time exhibits a super-Arrhenius decrease by decreasing T to near T_M , after which it slowly decays as it approaches the supercooled regime. The initial decrease in correlation time τ_c is similar to that of T_1 . It changes from ~ 1.3 ns, when $T_1 \sim 4.7$ s at 312 K, to ~ 0.3 ns, when $T_1 \sim 1.7$ s at 273 K.

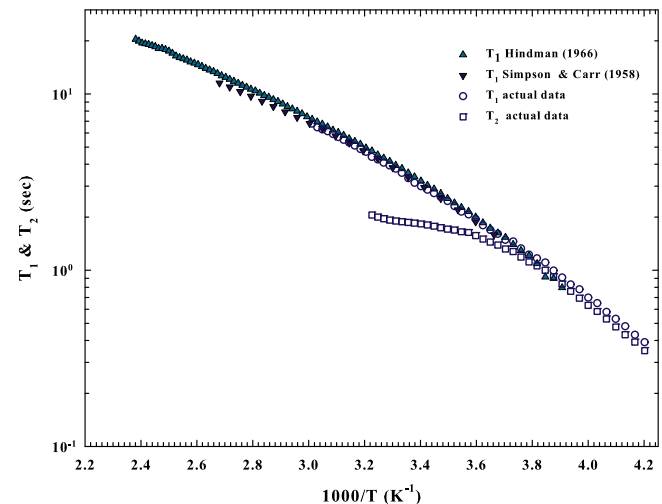


FIG. 1. Arrhenius plot of the NMR spin-lattice, T_1 , and spin-spin T_2 relaxation times. Open symbols represent actual data whereas the others refer to literature.^{30,31}

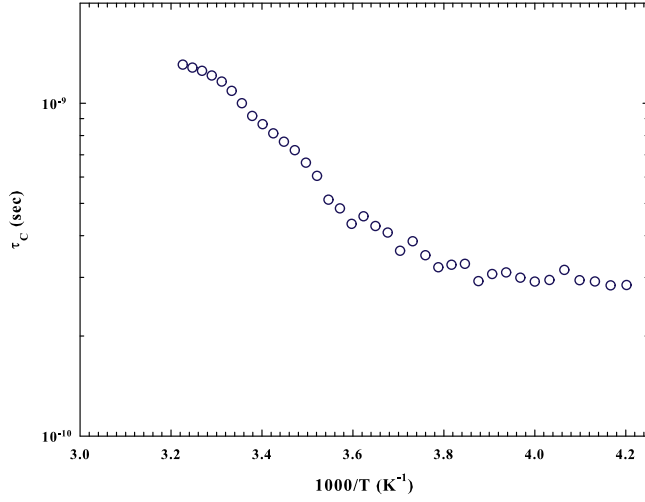


FIG. 2. The BPP correlation time τ_c calculated from these experimental values of T_1 and T_2 .

According to the BBP model, the temperature behavior of τ_c is caused by the evolution of the water structure. It is largely disordered at high T ($T > T^*$ ¹¹) and evolves toward a stable network at the supercooled phase.^{1,32,33} The water polymorphism of the SF and the LLPT models suggests that the onset of this “percolation-like” structure occurs in the stable liquid phase and becomes complete at the so-called Widom line,³⁴ which at the ambient pressure of our experiment is ≈ 225 K.^{32,35,36} NMR experiments focus on the local arrangement of the spin system, and the correlation time behavior reflects the dynamic effects of the water structure with its tetrahedral network formed by the HBs.

Figure 3 shows T_1 and T_2 as a function of the BPP correlation time τ_c . Note that although T_1 increases as the correlation time increases across the studied range, T_2 in the high τ_c regime remains nearly constant. Because we worked at $\omega_0 = 700$ MHz in order to satisfy the condition $1/\omega_0 = 1.429 \times 10^{-9} \gg \tau_c$, we are able to see the hyperbolic behaviors in the supercooled regime $T_2\tau_c \sim \text{const.}$ and $T_2 \approx T_1$ predicted by BPP, which is where the HB network becomes increasingly stable.

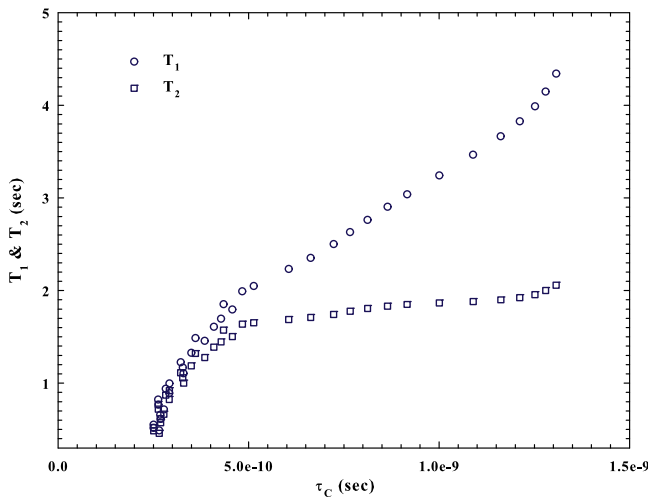


FIG. 3. The figure illustrates the behaviors of T_1 and T_2 as a function the correlation time τ_c .

Note that the behavior of both the NMR relaxation times T_1 and T_2 (when the temperature is increased) and the BPP correlation time is due to the local water order that is unstable at moderate temperatures above T_M , and that the instability increases as T increases. When a certain temperature is reached, the disordered HDL phase dominates the network structure of water and the degrees of freedom increase as T increases.^{32,33} Thus the time needed to restore equilibrium after the magnetic field has been applied increases, but the spin-spin relaxation time remains nearly constant. These NMR experiments probe how the onset of the tetrahedral HB water network is affected by supercooling to its “melting” point in the moderate high temperature regime near T^* . This is also confirmed by the fact that the HB lifetime becomes very short and its probability of forming becomes very low at these temperatures. This is important in chemistry and physics and in the technology of water solutions in which the HB interaction affects properties in competition with other interactions, e.g., ionic and hydrophobic. Of special interest here is how hydrophilicity (HB) and hydrophobicity have opposite effects on the folding and unfolding of biomolecules in water that influence the biological activity.

Using the Kubo and Tomita observation that the secular and non-secular spin lattice relaxations are not identical and that the different J_N spectral functions are characterized by different τ_i , Powles and Hubbard study the spin-lattice relaxation^{37,38} by assuming that three factors contribute to proton relaxation, intermolecular dipolar, intramolecular dipolar, and nuclear spin-rotation interactions. Thus

$$\frac{1}{T_1} = \frac{1}{T_1^D} + \frac{1}{T_1^{SR}} = \frac{1}{T_1^{D-Inter}} + \frac{1}{T_1^{D-Intra}} + \frac{1}{T_1^{SR}}. \quad (4)$$

Note that usually the rotational nuclear interaction is smaller than the dipolar interaction. It can be evaluated in water only when $T \geq 350$ K, where the system dynamics are strongly affected in the region of the critical point,³⁰

$$\frac{1}{T_1} = \frac{1}{T_1^D} = \frac{1}{T_1^{D-Inter}} + \frac{1}{T_1^{D-Intra}}. \quad (5)$$

Hubbard³⁸ proposed that the intermolecular dipolar contribution is strongly affected by the molecular self-diffusion coefficient D_S ,

$$\frac{1}{T_1^{D-Inter}} = \frac{N\pi\gamma^4\hbar^2}{5aD_S} \left[[1 + 0.233(b/a)^2 + 0.15(b/a)^4 \dots] \right], \quad (6)$$

where N is the number density of the nuclei, a is the hydrodynamic radius, and b is the distance of the nucleus from the center of the molecule. Having $D_S(T)$ in the same temperature range as the T_1 data reported in Fig. 1, we use this latter form to calculate $T_1^{D-Inter}$ for both the bulk and the emulsified water and use the values $a = 1.38$ Å and $b = 0.92$ Å^{39,40} (see the Arrhenius plot in Fig. 4).

Thus the difference between this latter quantity and T_1 allows us to obtain the intramolecular dipolar contribution (see Fig. 4). When $1/\omega_0 \gg \tau_i$ this can be written in terms of system viscosity η or molecular rotational time τ_θ ,^{27,39-41}

$$\frac{1}{T_1^{D-Intra}} = \frac{1}{T_1} - \frac{1}{T_1^{D-Inter}} = \frac{3\gamma^4\hbar^2}{2r^6} \tau_\theta. \quad (7)$$

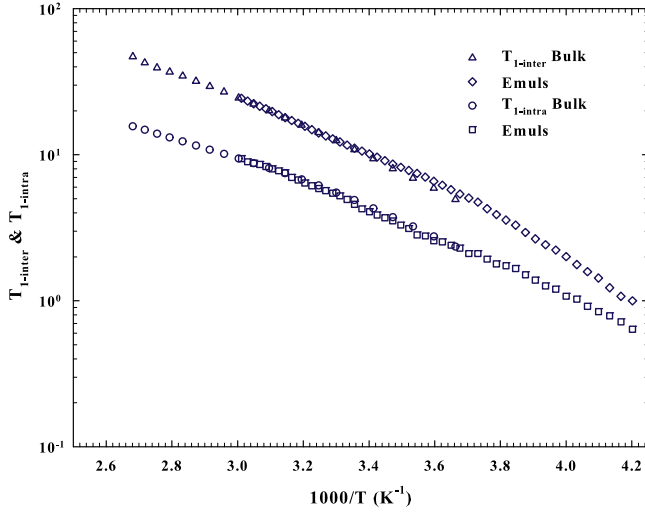


FIG. 4. The intermolecular and the intramolecular dipolar relaxations $T_1^{D-Inter}$ and $T_1^{D-Intra}$ are reported in an Arrhenius plot.

Figure 5 shows the calculated τ_θ ($r = 1.52 \text{ \AA}$) which we obtain and the data from the literature. The values from high temperatures to supercooled temperatures range within approximately one order of magnitude from 0.5 ps to 20 ps and their behavior is non-Arrhenius. Figure 5 also shows the viscosity η ⁴² and the relaxation time τ_R in the same temperature range in bulk water measured by depolarized Rayleigh scattering (DRS). η and τ_R are scaled using a multiplicative factor, 3 for τ_R and 3.155×10^{-12} for the viscosity measured in *cP*.^{43,44} Note that this relaxation process, related to the fast HB rearrangement at picosecond time scales, is rotational, and can be characterized as a HB breaking mechanism,^{45,46} therefore as a measure of the average water HB lifetime. Note also that the Raman DRS spectrum is a measure of the relaxation of the polarizability anisotropy, including rotational and translational molecular motions and their cross contributions. There are different ways of treating these data. The usual approach is that of the ideal mode coupling theory (MCT),⁴⁷

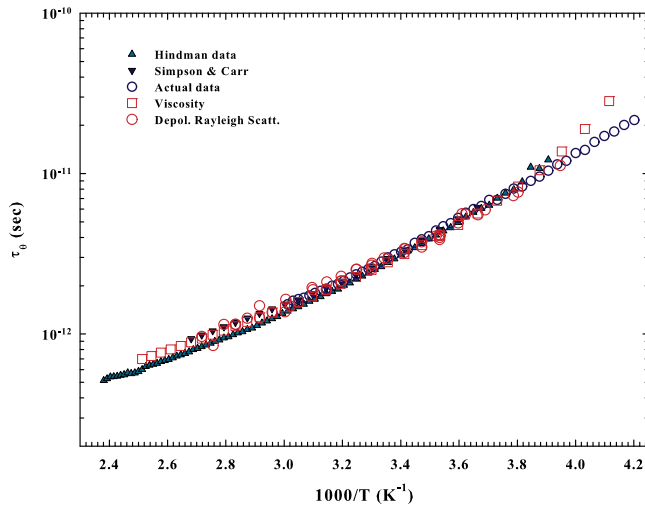


FIG. 5. The molecular rotational time τ_θ evaluated according to the Hubbard approach^{37,38} from the spin-lattice relaxation time, present and literature data. In the figure are also reported viscosity and depolarized Rayleigh scattering (DRS) data and relaxation time τ_R data^{43,44} normalized by means of a constant numerical factor.

$\tau(T) = a(T - T_c)^{-\gamma}$, where T_c is the ideal critical temperature and γ a non-universal exponent.⁴⁸ All the water transport parameter data (the viscosity, the self-diffusion coefficient, and the different relaxation times) obey this MCT power law, from the stable liquid phase to inside the supercooled region, giving $T_c \sim 221 \text{ K}$ and $\gamma \approx 2.2$.⁴⁹ This scenario has been also confirmed by different molecular dynamics simulation studies.¹ However, liquid bulk water cannot be easily studied below the homogeneous nucleation temperature $T_H = 231 \text{ K}$. The glass transition temperature of water is estimated to be $T_g \sim 130 \text{ K}$, and above that temperature it becomes a highly viscous fluid that crystallizes at $T_X \sim 150 \text{ K}$. On these bases there is the suggestion that liquid bulk water cannot be experimentally tested within the range from T_H to T_X , the so-called No Man's Land. However, such a constrain has been overcome by using confined water^{32,35,36} and recently in micrometer water droplets with a diameter of 9 or 12 μm .⁵⁰ In the first case, temperatures up to about 190 K can be explored, whereas in the second one the minimum reached temperature was 227 K. It must be noticed that all the measured dynamical data are substantially, in both cases, in good agreement.

All the $\tau_\theta(T)$ data shown in Fig. 5 are measured inside the bulk liquid phase and obey the MCT power law with an estimated exponent γ and a T_c that, within experimental error, are the same as the other water transport parameters.

Angell and Ito⁵¹ use a power law approach similar to MCT to study the water relaxation time; the transition from fragile (super-Arrhenius) to strong (Arrhenius) at $T_L \sim 221 \text{ K}$ is caused by the growth of the water LDL network when T is decreased.^{33,51} Instead in a previous paper, Speedy and Angell proposed by using the same power law for the compressibility data a divergence at 228 K.⁴ This fragile-to-strong dynamical crossover has been observed in many molecular glass forming liquids in the bulk phase,^{49,52} but not in water because of the No Man's Land where it can only be studied under confinement.^{6,35,53} The MCT explains this in terms of molecular hopping^{49,54} that occurs between the HB water clusters corresponding to hopping between energy basins in an energy landscape. The inherent structures describing the supercooled liquid state of glass-forming materials have been developed for water.⁵⁵

Although we have studied bulk and emulsified water far from T_c (our limit is 238 K), we also explore the supercooled regime within a temperature interval where the HB network dominates system dynamics. Figure 6 shows how the NMR relaxation times as a function of τ_θ accurately describe the HB effect on water. Figure 6 also shows the differing behaviors above and below $\tau_\theta \approx 7.5 \text{ ps}$ (the value for $T \approx 266 \text{ K}$). For $T < 266 \text{ K}$ the spin-lattice and the spin-spin relaxation times have the same behavior, a power law as a function of τ_θ , T_1 , and $T_2 \sim \tau_\theta^{-\Delta}$, with $\Delta \approx 1.1$ (solid line). When $T > 266 \text{ K}$ and $\tau_\theta < 7.5 \text{ ps}$; however, these two characteristic NMR times behave differently. The T_1 values again show power law behavior, there is a little change in slope $\Delta \approx 0.9$ (dotted line), and T_2 slowly evolves toward the high temperature regime. The behavior inside the supercooled regime indicated by the power law index exhibits a consistent correlation between the three NMR relaxation times (T_1 , T_2 , and τ_θ) and occurs because there is a water structure with stable HBs. Instead when the

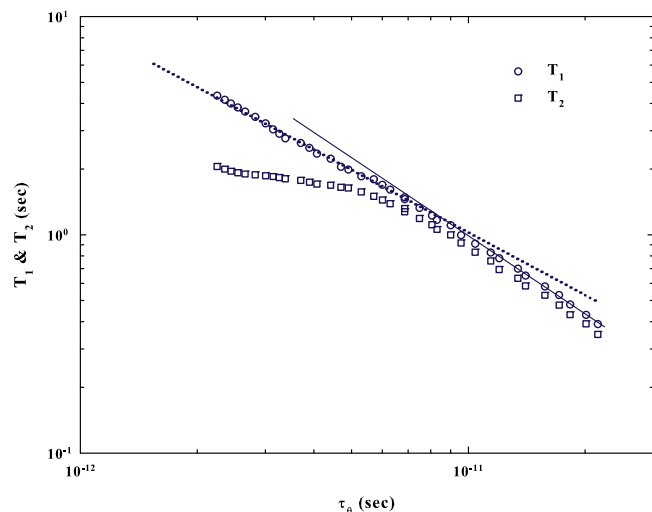


FIG. 6. A log-log plot of the NMR relaxation times T_1 and T_2 versus the rotational time τ_θ .

temperature becomes so high that the water network melts and the rotational correlation time τ_θ approaches the values of the order of some picoseconds, the spin-spin and the spin-lattice times must evolve differently with a sort of decoupling in the translational and rotational dynamics.

III. CONCLUSIONS

We have investigated the dynamic behavior of water as a function of temperature across a wide range—including the supercooled regime for both bulk and the emulsified water—using NMR spectroscopy, and have observed the evolution of the spin-lattice and spin-spin relaxation times. The data we obtain agree well within error bars with literature data. To explore the influence of HB interactions on water properties, we use two different approaches to determine how the motion of a given proton in a water molecule is determined by its nearest neighbors. In the first case, we use the classical approach of a single characteristic correlation time τ_c caused by the thermal motion effects of the magnetic nuclei on the spin-spin interaction. Figure 3 shows how the temperature evolutions of T_1 and T_2 as a function of τ_c can be used to explain how the HB interactions create the characteristic tetrahedral transient network and make water polymorphism the cause of system thermodynamical anomalies. In the second case, we use a model developed by Hubbard in the same theoretical scheme (BPP and Kubo-Tomita) that uses spin-lattice time relaxation and transport parameter data (viscosity or self-diffusion) to evaluate the rotational time τ_θ of a proton. Note that τ_θ is related to spin-spin rotational correlations and has the same thermal behavior as other liquid water transport parameters such as viscosity and rotational (DRS) relaxation time. Here also the correlations of NMR relaxations T_1 and T_2 with measured τ_θ are evidence that HB interactions determine water properties and dynamics. In the supercooled regime, these relaxation times are strongly correlated because the HB interactions are strong enough and have a lifetime long enough to sustain a stable water network, but a temperature increase decreases the HB interaction lifetime and eventually destroys the water clusters and decouples the dynamic modes of the

system. Our results indicate that when HB interactions that facilitate clustering in water solutions compete with interactions with opposite behaviors, e.g., hydrophobicity, the effects of these latter interactions become relevant for temperatures where the water tetrahedral network is no longer stable.

ACKNOWLEDGMENTS

The D.M.'s activity is carried out within the framework of the NANORESTART project which has received funding from the European Union's Horizon 2020 research and innovation programme under Grant Agreement No. 646063. The Boston University work was supported by DTRA Grant No. HDTRA1-14-1-0017, by DOE Contract No. DE-AC07-05Id14517, and by NSF Grant Nos. CMMI 11-25290, PHY 15-05000, and CHE-1213217.

- ¹H. E. Stanley, in *Liquid Polymorphism*, edited by S. A. Rice (Wiley, New York, 2013).
- ²P. G. Debenedetti and H. E. Stanley, *Phys. Today* **56**(6), 40 (2003).
- ³C. A. Angell, in *Water: A Comprehensive Treatise*, edited by J. Straub and K. Scheffler (Pergamon, Elmsford, NY, 1982), Vol. 7, pp. 261–271.
- ⁴R. J. Speedy and C. A. Angell, *J. Chem. Phys.* **65**, 851 (1976).
- ⁵P. G. Debenedetti, *Metastable Liquids* (Princeton University Press, Princeton, 1997).
- ⁶F. Mallamace, P. Baglioni, C. Corsaro, J. Spooren, H. E. Stanley, and S.-H. Chen, *Riv. Nuovo Cimento* **34**, 253 (2011).
- ⁷F. Mallamace, C. Corsaro, D. Mallamace, P. Baglioni, H. E. Stanley, and S.-H. Chen, *J. Phys. Chem. B* **115**, 14280 (2011).
- ⁸F. Mallamace, C. Corsaro, S.-H. Chen, and H. E. Stanley, *Adv. Chem. Phys.* **152**, 203 (2013).
- ⁹F. Mallamace, C. Corsaro, D. Mallamace, S.-H. Chen, and H. E. Stanley, *Adv. Chem. Phys.* **152**, 263 (2013).
- ¹⁰P. Kumar and H. E. Stanley, *J. Phys. Chem.* **115**, 14269 (2011).
- ¹¹F. Mallamace, C. Corsaro, and H. E. Stanley, *Sci. Rep.* **2**, 993 (2012).
- ¹²Y. Levy and J. Onuchic, *Annu. Rev. Biophys. Biomol. Struct.* **35**, 389415 (2006).
- ¹³G. A. Jeffrey and W. Saenger, *Hydrogen Bonding in Biological Structures* (Springer-Verlag, Berlin, 1991).
- ¹⁴F. Mallamace, C. Corsaro, D. Mallamace, S. Vasi, C. Vasi, P. Baglioni, S. V. Buldyrev, S. H. Chen, and H. E. Stanley, *Proc. Natl. Acad. Sci. U. S. A.* **113**, 3159 (2016).
- ¹⁵N. Bloembergen, E. M. Purcell, and R. V. Pound, *Phys. Rev.* **73**, 679 (1948).
- ¹⁶R. Kubo and K. Tomita, *J. Phys. Soc. Jpn.* **9**, 888 (1954).
- ¹⁷F. Mallamace, *Proc. Natl. Acad. Sci. U. S. A.* **106**, 15097 (2009).
- ¹⁸H. E. Stanley, P. Kumar, G. Franzese, L. Xu, Z. Yan, M. G. Mazza, S. V. Buldyrev, S. H. Chen, and F. Mallamace, *Eur. Phys. J. Spec. Top.* **161**, 1 (2008).
- ¹⁹O. Mishima, *Nature* **384**, 546 (1996).
- ²⁰O. Mishima, L. D. Calvert, and E. Whalley, *Nature* **314**, 76 (1985).
- ²¹O. Mishima, L. D. Calvert, and E. Whalley, *Nature* **310**, 393 (1984).
- ²²H. E. Stanley, *J. Phys. A: Math. Gen.* **12**, L329 (1979).
- ²³H. E. Stanley and J. Texeira, *J. Chem. Phys.* **73**, 3404 (1980).
- ²⁴A. Geiger and H. E. Stanley, *Phys. Rev. Lett.* **49**, 1749 (1982).
- ²⁵J. R. Errington, P. G. Debenedetti, and S. Torquato, *Phys. Rev. Lett.* **89**, 215503 (2002).
- ²⁶O. Mishima, *J. Chem. Phys.* **133**, 3496 (2010).
- ²⁷E. W. Lang and H.-D. Ludemann, *J. Chem. Phys.* **67**, 718 (1977).
- ²⁸A. Abragam, *The Principles of Nuclear Magnetism* (Oxford, Oxford, UK, 1961).
- ²⁹F. Bloch, *Phys. Rev.* **70**, 460 (1946).
- ³⁰J. C. Hindman, *J. Chem. Phys.* **44**, 4582 (1966).
- ³¹J. H. Simpson and H. Y. Carr, *Phys. Rev.* **111**, 1201 (1958).
- ³²F. Mallamace, M. Broccio, C. Corsaro, A. Faraone, D. Majolino, V. Venuti, L. Liu, C. Y. Mou, and S. H. Chen, *Proc. Natl. Acad. Sci. U. S. A.* **104**, 424 (2007).
- ³³L. Xu, F. Mallamace, Z. Yan, F. Starr, S. V. Buldyrev, and H. E. Stanley, *Nat. Phys.* **5**, 565 (2009).
- ³⁴L. Xu, P. Kumar, S. V. Buldyrev, S.-H. Chen, P. H. Poole, F. Sciortino, and H. E. Stanley, *Proc. Natl. Acad. Sci. U. S. A.* **102**, 16558 (2005).

- ³⁵L. Liu, S. H. Chen, A. Faraone, C. Yen, and C. Y. Mou, *Phys. Rev. Lett.* **95**, 117802 (2005).
- ³⁶S. H. Chen, F. Mallamace, C. Y. Mou, M. Broccio, C. Corsaro, A. Faraone, and L. Liu, *Proc. Natl. Acad. Sci. U. S. A.* **103**, 12974 (2006).
- ³⁷D. W. G. Smith and J. C. Powles, *Mol. Phys.* **10**, 451 (1966).
- ³⁸P. S. Hubbard, *Phys. Rev.* **131**, 275 (1963).
- ³⁹T. De Fries and J. Jonas, *J. Chem. Phys.* **66**, 896 (1977).
- ⁴⁰J. Jonas, T. De Fries, and D. J. Wilbur, *J. Chem. Phys.* **65**, 582 (1976).
- ⁴¹F. X. Prielmeier, E. W. Lang, R. J. Speedy, and H. D. Ludemann, *Phys. Rev. Lett.* **59**, 1128 (1987).
- ⁴²C. H. Cho, J. Urquidi, S. Singh, and G. W. Robinson, *J. Phys. Chem. B* **103**, 1991 (1999).
- ⁴³M. Paolantoni, P. Sassi, A. Morresi, and S. Santini, *J. Chem. Phys.* **127**, 024504 (2007).
- ⁴⁴V. Mazzacurati, A. Nucara, M. A. Ricci, G. Ruocco, and G. Signorelli, *J. Chem. Phys.* **93**, 7767 (1990).
- ⁴⁵F. Aliotta, C. Vasi, G. Maisano, D. Majolino, F. Mallamace, and P. Migliardo, *J. Chem. Phys.* **84**, 4731 (1986).
- ⁴⁶N. Micali, S. Trusso, C. Vasi, D. Blaudez, and F. Mallamace, *Phys. Rev. E* **54**, 1720 (1996).
- ⁴⁷A. P. Sokolov, J. Hurst, and D. Quitmann, *Phys. Rev. B* **51**, 12865 (1995).
- ⁴⁸W. Goetze and L. Sjoegren, *Rep. Prog. Phys.* **55**, 241 (1992).
- ⁴⁹F. Mallamace, C. Branca, C. Corsaro, N. Leone, J. Spooren, S. H. Chen, and H. E. Stanley, *Proc. Natl. Acad. Sci. U. S. A.* **107**, 22457 (2010).
- ⁵⁰J. A. Sellberg, A. F. Huang, T. A. McQueen, N. D. Loh, H. Laksmono, D. Schlesinger, R. G. Sierra, D. Nordlund, C. Y. Hampton, D. Starodub, D. P. Deponte, M. Beye, C. Chen, A. Martin, A. Barty, K. T. Vikfeldt, T. Weiss, C. Caronna, J. Feldkamp, B. L. Skinner, M. M. Seibert, M. Messerschmidt, G. J. Williams, S. Boutet, L. G. M. Petterson, M. J. Bogan, and A. Nilsson, *Nature* **510**, 381 (2009).
- ⁵¹K. Ito, C. T. Moynihan, and C. A. Angell, *Nature* **398**, 492 (1999).
- ⁵²F. Mallamace, C. Corsaro, N. Leone, V. Villari, N. Micalii, and S. H. Chen, *Sci. Rep.* **4**, 3747 (2014).
- ⁵³S. Cervený, F. Mallamace, J. Swenson, M. Vogel, and L. M. Xu, *Chem. Rev.* **116**, 7608 (2016).
- ⁵⁴S. H. Chong, S. H. Chen, and F. Mallamace, *J. Phys.: Condens. Matter* **21**, 504101 (2009).
- ⁵⁵F. Stillinger, *Energy Landscapes, Inherent Structures, and Condensed-Matter Phenomena* (Princeton University Press, Princeton, 2016).